ACS POLYMERS Au
AN OPEN ACCESS JOURNAL OF THE AMERICAN CHEMICAL SOCIETY

pubs.acs.org/polymerau

Article

Electronic and Magnetic Properties of a Three-Arm Nonconjugated Open-Shell Macromolecule

Hyunki Yeo, Siddhartha Akkiraju, Ying Tan, Hamas Tahir, Neil R. Dilley, Brett M. Savoie, and Bryan W. Boudouris*

Cite This: *ACS Polym. Au* 2022, 2, 59–68

Read Online

ACCESS | Metrics & More | Article Recommendations | Supporting Information

ABSTRACT: Nonconjugated radical polymers (i.e., macromolecules with aliphatic backbones that have stable open-shell sites along their pendant groups) have arisen as an intriguing complement to π-conjugated polymers in organic electronic devices and may prove to have superior properties in magneto-responsive applications. To date, however, the design of nonconjugated radical polymers has primarily focused on linear homopolymer, copolymer, and block polymer motifs even though conjugated dendritic macromolecules (i.e., polyradicals) have shown significant promise in terms of their response under applied magnetic fields. Here, we address this gap in creating a nonconjugated, three-arm radical macromolecule with nitroxide open-shell sites using a straightforward, single-step reaction, and we evaluated the electronic and magnetic properties of this material using a combined computational and experimental approach. The synthetic approach employed resulted in a high-purity macromolecule with a well-defined molecular weight and narrow molecular weight distribution. Moreover, epoxide-based units were implemented in the three-arm radical macromolecule design, and this resulted in a nonlinear radical macromolecule with a low (i.e., below room temperature) glass transition temperature and one that was an amorphous material in the solid state. These properties allowed thin films of the three-arm radical macromolecule to have electrical conductivity values on par with many linear radical polymers previously reported, and our computational efforts suggest the potential of higher generation open-shell dendrimers to achieve advanced electronic and magnetic properties. Importantly, the three-arm radical macromolecule also demonstrated antiferromagnetic exchange coupling between spins at temperatures < 10 K. In this way, this effort puts forward key structure−property relationships in nonlinear radical macromolecules and presents a clear path for the creation of next-generation macromolecules of this type.

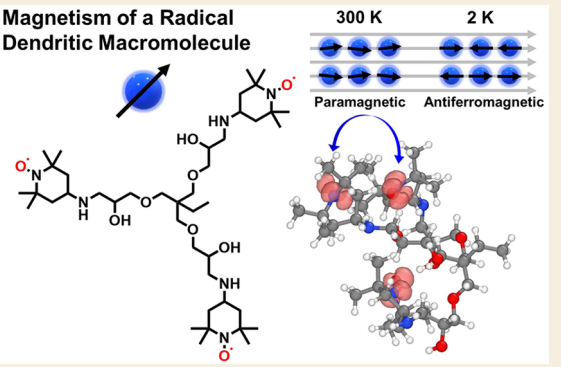

KEYWORDS: *Open-shell macromolecules, Nitroxide-containing macromolecules, Conducting dendrimers, Radical dendrimers, Magnetic macromolecules*

INTRODUCTION

Since their initial discovery, the development of organic electronic molecules has led to materials with impressive optoelectronic, thermoelectric, and bioelectronic performance.[1−6] Moreover, the ability to tune the properties of electronic polymers using straightforward organic chemistry design strategies has allowed for the refinement of both their mechanical properties and their end-use device performance in a ready manner.[7−10] As such, the polymer electronics community has made impressive strides in applications ranging from energy conversion and storage systems to materials that are used in health monitoring devices.[11−14] In most of these applications, π-conjugated polymers have been implemented as their molecular architecture can facilitate charge delocalization (i.e., through conjugation) and relatively ordered packing (i.e., in driving crystallization of the macromolecules), which typically improves charge transport across macroscopic distances.[15,16] However, these conjugated polymers have not shown as much success in magnetic-field-dependent applications relative to electronic applications due to the singlet ground state of their electronic configurations and their diamagnetic nature.[17−19] As a result, researchers have transitioned to molecules containing stable open-shell entities to push this important area forward.[20,21] That is, these open-shell molecules contain robust spin sites and offer more promise for magnetic field-dependent applications. In fact, several classes of molecules containing one or more radicals have been reported.[22−25] One material group, polyradicals, has shown strong magnetic properties due to the large number of

Received: August 23, 2021
Revised: October 12, 2021
Accepted: October 27, 2021
Published: November 15, 2021

https://doi.org/10.1021/acspolymersau.1c00026
ACS Polym. Au 2022, 2, 59–68

open-shell sites within a single repeat unit.[26,27] This architecture facilitates interactions between the unpaired electrons, resulting in strong antiferromagnetic or ferromagnetic behavior. While these polyradicals show strong magnetic properties, their syntheses are often quite complicated, which limits their translational potential. Therefore, other alternative polymeric designs that offer more straightforward synthetic handles while retaining the open-shell character have been developed.[28−31]

For instance, linear radical polymers are composed of a nonconjugated backbone with stable open-shell pendant groups, and they have shown great promise in electronic and electrochemical applications due to their tunable molecular design and relatively simple syntheses.[32,33] As a result, they have been widely used in several emerging applications (e.g., flexible batteries).[34−41] However, early work on the magnetic properties of these radical polymers showed weak magnetic interactions between the open-shell sites.[42−44] Unlike polyradicals, radical polymers have only a single unpaired electron per repeat unit and they are usually completely amorphous in the solid state, which can limit spin ordering. Additionally, while radical polymers contain a large number of open-shell sites as a whole, the distance between these sites is much larger than that in polyradicals. This prevents the spins from interacting in a coherent manner, and this, in turn, inhibits strong magnetic interactions. Therefore, it is imperative to expand the field of radical-containing polymers to evaluate macromolecular architectures that are nonlinear in nature.[45−49]

As a starting point for these next-generation designs, it is useful to recall that the tailored design of a specific radical polymer, poly(4-glycidyloxy-2,2,6,6-tetramethylpiperidine-1-oxyl) (PTEO), led to a pristine (i.e., not doped) linear radical polymer that exhibited high solid-state electronic conductivity values (~10 S m^{-1}) due to the local ordering of the pendant radical groups along the polymer when thin films of PTEO were annealed above the glass transition temperature (T_g) and below the degradation temperature (T_d) of the radical polymer.[50] Here, we extend this line of thinking to move beyond linear radical polymers and instead determine how the local order of open-shell entities along a three-arm radical macromolecule allows for control of both its electronic and magnetic environment. That is, we will continue to utilize the 2,2,6,6-tetramethylpiperidine-1-oxyl (TEMPO) open-shell chemistry within the polymer design due to its previous success in the linear radical polymer regime.[51−54] The shift to a dendritic macromolecular architecture was implemented because dendrimers allow for ready control over their macromolecular structure and impart a natural means by which to synthesize macromolecules with nearly uniform molecular weight distributions. This feature is anticipated to be important in controlling the magnetic order within the materials.[55] In fact, inorganic magnetically active dendrimers have been reported previously, and they have shown impressive electronic and magnetic performance.[56−58] Moreover, many polyradical species have a dendrimer-like structure as well; however, their units are intentionally designed to be conjugated to one another such that there is inherent intramolecular communication between the open-shell sites. Here, we couple these paradigms with our own "low-T_g" approach from the PTEO linear radical polymer work to establish the electronic and magnetic behavior nonconjugated radical dendrimers.

In this way, this work takes advantage of these structure−property patterns to develop a new open-shell dendritic macromolecule, a trinitroxide version of 4,4′-((((2-ethyl-2-((2-hydroxy-3-((1-hydroxy-2,2,6,6-tetramethylpiperidin-4-yl)-amino)propoxy)methyl)propane-1,3-diyl)bis(oxy))bis(2-hydroxypropane-3,1-diyl))bis(azanediyl))bis(2,2,6,6-tetramethylpiperidin-1-ol) (E1-TEMPO). E1-TEMPO is a three-arm nonconjugated open-shell macromolecule synthesized through a straightforward amine−epoxy reaction without the use of a catalyst.[59−62] Furthermore, the low glass transition temperature (i.e., T_g = −20 °C) led to ordering in thin films of E1-TEMPO. These thin films exhibited relatively high electronic conductivity values that were independent of temperature and in agreement with previous reports for linear radical polymers with similar chemical design motifs.[63−65] Although the current conductivity values of E1-TEMPO are approximately the same compared to many of their linear radical polymer analogues, the key computational results indicate the potential for higher generation open-shell dendrimers to have advanced electronic and magnetic properties relative to the current state-of-the-art linear polymers. Computational studies of E1-TEMPO showed this nonlinear construct allowed for radical localization while still supporting intra- and intermolecular open-shell interactions. Through these interactions, E1-TEMPO demonstrated clear antiferromagnetic interactions, which has not been reported for dendritic nonconjugated radical macromolecular materials. Furthermore, the simulation results suggest that, when translated to higher-generation dendrimers, the intrachain spin interactions will be promoted while maintaining the interchain interactions. Therefore, this work serves as a template for developing structure−property relationships of open-shell dendritic macromolecules and expanding the field of organic magnetic materials in a straightforward manner.

EXPERIMENTAL SECTION

Materials

Trimethylolpropane triglycidyl ether (E1) and 4-amino-2,2,6,6-tetramethylpiperidine-1-oxyl (4-amino-TEMPO) were purchased from Sigma-Aldrich. All chemicals were used as they were received. Tin-doped indium oxide-coated (ITO-coated) glass substrates were purchased from Delta Technologies, Inc.

General Methods

Proton (^{1}H) and carbon (^{13}C) nuclear magnetic resonance (NMR) spectra were collected using a Bruker Avance III HD 400-MHz NMR spectrometer. Chemical shifts of the signals were reported relative to a tetramethylsilane (TMS) standard. To allow for proper data collection, the radical sites of the E1-TEMPO macromolecule were quenched using a 5% (by weight) HCl in methanol solution prior to the spectra being acquired. In these measurements, E1 and E1-TEMPO were dissolved in deuterated dimethyl sulfoxide (DMSO) at a concentration of 1 mg mL^{-1}. High resolution mass spectroscopy data of E1-TEMPO were collected using an Advion mass spectrometer in an anhydrous chloroform solution at a concentration of 1 mg mL^{-1}. Fourier transform infrared (FTIR) spectra were obtained using a Thermo Nicolet Nexus 670 Fourier transform infrared spectrophotometer. Electron paramagnetic resonance (EPR) spectra were acquired at room temperature using a Bruker EMXEPR spectrometer. To make the solutions for EPR spectroscopy measurements, 4-amino-TEMPO and E1-TEMPO were dissolved in anhydrous chloroform at a concentration of 1 mg mL^{-1}. The molecular weight and dispersity of the E1-TEMPO macromolecule was characterized by size exclusion chromatography (SEC) using a Hewlett-Packard 1260 Infinity series instrument. Polystyrene standards (Agilent Easi Cal) of molecular weight values ranging from 1 to

https://doi.org/10.1021/acspolymersau.1c00026
ACS Polym. Au 2022, 2, 59−68

200 kg mol^{-1} were utilized to calibrate the SEC. The mobile phase was tetrahydrofuran (THF) at a temperature of 35 °C and a flow rate of 1 mL min^{-1}. Differential scanning calorimetry (DSC) data were collected using a TA Instruments Q20 Series differential scanning calorimeter, and these experiments were performed under a nitrogen environment at a gas flow rate of 50 mL min^{-1}. E1-TEMPO was initially heated to 75 °C, held isothermally for 30 min, then cooled to −50 °C, and then held isothermally for 5 min. Then, the sample was heated again, and the glass transition temperature was acquired from this scan. All heating and cooling ramps occurred at the rate of 10 °C min^{-1}. Thermogravimetric analysis (TGA) data were collected using a TA Instruments Q600 SDT Series simultaneous thermal analyzer, and the experiments were performed under a helium environment at a gas flow rate of 100 mL min^{-1}. E1-TEMPO was initially held isothermal for 30 min at 20 °C, then heated to 800 °C at a rate of 10 °C min^{-1}.

Synthesis of E1-TEMPO

In this reaction, 1.2 g (7.01 mmol) of 4-amino-TEMPO was added to 0.59 g (1.95 mmol) of E1 dissolved in 5 mL of tetrahydrofuran. Then, the mixture was stirred at 50 °C for 24 h in ambient conditions. The residual THF was evaporated, and the crude product was purified by silica gel column chromatography with an eluent of dichloromethane and methanol at a volumetric ratio of 95:5. The organic solvents were removed under reduced pressure, and the product, E1-TEMPO, was dried overnight in a vacuum oven. This yielded 1.4 g (yield = 88%) of E1-TEMPO, and the molecule was obtained in the form of viscous orange-red liquid at room temperature. ^{1}H NMR (400 MHz, DMSO-d_6) δ 11.49 (s, 3H), 8.39 (s, 6H), 3.80 (s, 15H), 3.46−3.23 (m, 6H), 2.92−2.81 (m, 3H), 2.35−1.99 (m, 12H), 1.56−1.13 (m, 38H), 0.81 (dd, J = 9.8, 5.5 Hz, 3H). ^{13}C NMR (400 MHz, DMSO-d6) δ 67.12, 41.06, 27.38, 21.56, 20.14, 7.72. HRMS (APCI+) m/z calculated for $C_{42}H_{84}O_9N_6$ [M]$^+$: 816.62943, observed: 816.62991. M_n (SEC vs PS standards) = 618 g mol^{-1}; $Đ$ = 1.04.

Computational Methods

Molecular dynamics (MD) simulations were used to characterize and compare the radical distributions in the first-generation and second-generation radical dendrimers, E1-TEMPO and E2-TEMPO, respectively. Due to the relatively slow time scale of conformational equilibration in macromolecules, a preliminary conformational relaxation was performed prior to initializing the MD simulations. The simulation procedure was composed of an initial geometry optimization, CREST conformer search,[66,67] and GFN-FF based molecular dynamics simulations.[68] The initial geometry optimizations were preliminarily optimized via the universal force field (UFF)[69] in Avogadro,[70] followed by optimization at the semiempirical GFN2-xTB level.[71] Based on the initially optimized geometry, CREST was applied for 10 ps to identify the lowest energy conformer. For MD simulations, the lowest energy conformer of E1-TEMPO was duplicated 8 times and randomly oriented (total atom number of 1120 and 24 radical sites) and then placed at each corner of the cubic simulation cell with a box length of 3.7 nm while avoiding atomic overlaps. The lowest energy conformer of E2-TEMPO was duplicated 3 times with 1320 atoms and 27 radical sites in total. MD simulations were performed using GFN-FF force field as implemented in the xtb package. A single NVT trajectory was simulated for each system at each temperature, with a total run time of 500 ps per trajectory and an integration time step of 2 fs. The system was confined using a logfermi spherical potential. Configuration snapshots were sampled every 0.5 ps. To avoid a kinetically trapped, nonequilibrium simulation from the unequilibrated initial geometry, two different temperatures (i.e., one above and one below the experimentally measured glass transition temperature) were simulated (i.e., T = 233 and 273 K) to ensure the system reaches thermal equilibrium above the glass transition temperature. The last 50 snapshots generated by MD simulations have a number of density (radical monomer unit) of 1.05 × 10^{21} cm^{-3}. The atomic positions taken from these snapshots were further characterized by interchain, intrachain and total atom-type based radial distribution functions (RDFs) with a cutoff of 2 nm.

Device Fabrication and Electronic Conductivity Measurements

ITO-coated glass substrates were cleaned in acetone, chloroform, and isopropyl alcohol by sonication for 10 min each in a sequential order. E1-TEMPO was dissolved in chloroform at a concentration of 100 mg mL^{-1}. In air, the solutions were spin-coated on the ITO substrates at a rate of 2000 rpm for 60 s to form a layer that was ∼90 nm thick, as measured using a Bruker Dektak XT stylus profilometer. The films were annealed at 70 °C for 30 min to remove the residual solvent. The films were then placed in a thermal evaporator installed in inert atmosphere glovebox. Then, 20 nm of gold was deposited on top of the films at a reduced pressure of ∼10^{-6} bar to yield a device active area of 0.06 cm^2. Conductivity values were calculated by using a PS100 Lakeshore probe station with a Keithley 2400 source meter to control the voltage values in the range of -1 V $\leq V \leq +1$ V, by measuring the resistance values in vacuum from 20 to 80 °C in intervals of 10 °C.

Magnetism Measurements

The magnetic susceptibility of E1-TEMPO was measured using a superconducting quantum interference device (SQUID) magnetometer. The sample was zero-field cooled to 2 K. Afterward, a field of 0.5 T was applied and the magnetic susceptibility was measured from 2 to 300 K in intervals of 0.03 K. The magnetization of E1-TEMPO was measured using the same SQUID magnetometer. A field of -7 T $\leq B \leq +7$ T was applied to the sample and the moment was measured at T = 2, 3, 5, 10, and 20 K.

RESULTS AND DISCUSSION

The nitroxide radical functionality was selected for the three-arm macromolecule synthesis due to its known solid-state magnetic properties with distinct magnetic ordering at low temperature and its ability to conduct charge in the solid state.[31,72] Additionally, the TEMPO radical is relatively stable with respect to elevated temperatures, air exposure, and humidity conditions, which provided an advantage in terms of materials stability during this initial foray into nonconjugated three-arm radical macromolecules.[73] During the reaction to form E1-TEMPO (Figure 1a), the epoxide rings of a three-armed core, trimethylolpropane triglycidyl ether (E1), were opened by a three equivalent molar ratio of 4-amino-2,2,6,6-tetramethylpiperidine-1-oxyl (4-amino-TEMPO) with no additional reagents (Figure S1). This β-hydroxyl-amine bond formation allowed for the successful synthesis of the radical-containing macromolecule with the targeted molecule weight and a nearly uniform molecular weight distribution ($Đ$ = 1.04). In the epoxy precursor, E1, the stretches associated with the epoxide bonds at 839, 906, and 1093 cm^{-1} were observed using FTIR spectroscopy (Figure 1b). After the ring-opening reaction occurred, these signals were no longer present in the E1-TEMPO spectrum. Also, the N−H stretch at 3359 cm^{-1} was suppressed, and the N−H bend signals that appear exclusively in primary amines at 1598 cm^{-1} disappeared in the E1-TEMPO spectrum. Furthermore, an increase of the O−H stretch in the region around 3400 cm^{-1}, which belongs to the newly formed hydroxyl groups, was observed only in the E1-TEMPO spectrum.

Moreover, the ring-opening reaction of E1 was evaluated using ^{1}H NMR spectroscopy, which highlighted that the resonance signals from methylene groups adjacent to the nitrogen atoms were present at the expected chemical shifts of at 2.88 and 3.25 ppm relative to TMS (Figure 2). Also, the formation of newly formed β-hydroxyl-amine bonds could be quantified by the integration of signals of the protons from the amine group at a chemical shift of 11.49 ppm and the hydroxyl

https://doi.org/10.1021/acspolymersau.1c00026
ACS Polym. Au 2022, 2, 59−68

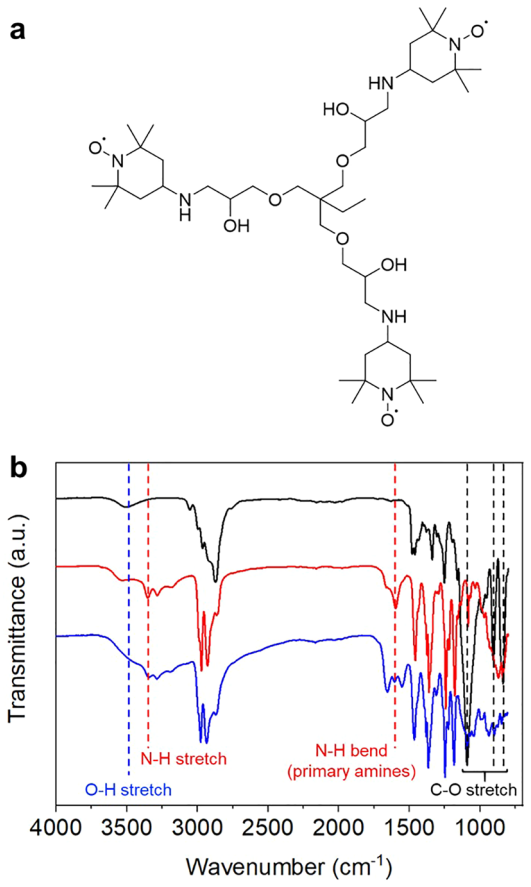

Figure 1. (a) Molecular structure of E1-TEMPO. (b) FTIR spectra of E1 (black), 4-amino-TEMPO (red), and E1-TEMPO (blue) highlighting the conversion of the precursor E1 to the desired E1-TEMPO product.

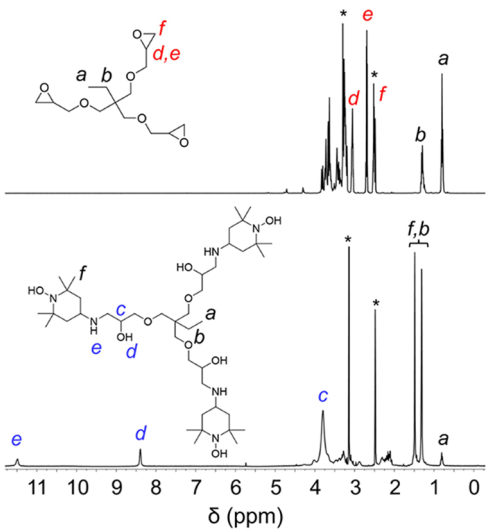

Figure 2. Comparison of the ^{1}H NMR spectra of the starting material, E1, and E1-TEMPO where the open-shell entities have been intentionally quenched using a methanol solution containing hydrochloric acid. The asterisk (*) notes the signal that occurs due to the presence of the deuterated DMSO solvent ($\delta \sim 2.5$ ppm) and residual water ($\delta \sim 3.3$ ppm).

group at a chemical shift of 8.39 ppm. Finally, the elimination of the signature signals associated with the protons of the epoxide groups at chemical shifts of 3.06, 2.69, and 2.52 ppm was observed, and this confirmed that all the epoxide rings opened during the reaction. Additionally, the ^{13}C NMR spectrum of the final product was consistent with the predicted signal (Figure S2), and the high-resolution mass spectrometry data agreed with the formation of the desired product as well. Thus, E1-TEMPO was synthesized successfully in a simple, single step with no side reactions, which provided a simple pathway for the evaluation of the structure−property relationships to be developed in this new type of magneto-responsive nonlinear radical macromolecule.

In addition to the molecular characteristics associated with the spectroscopic results shown above, the radical content of the E1-TEMPO macromolecule was found to be relatively high and the exchange interactions of these spin sites were evaluated using EPR spectroscopy. Specifically, the spectrum of E1-TEMPO showed an identical shape of 4-amino-TEMPO; that is, three maxima, with relative intensities of 1:1:1 from the coupling of the ^{14}N atoms (Figure 3a), were observed. The radical content of E1-TEMPO was 85% of all of the potential radical sites relative to 4-amino-TEMPO, which was used as the standard (Figure S3). The drop in radical content (i.e., relative to the 4-amino-TEMPO standard) is likely due to quenching of radicals during the reaction and not due to incomplete coupling between the amine and epoxy groups. While not reaching 100% radical density, the synthesized macromolecules possessed a high density of radical sites, which was similar to the starting material. Again, these data highlight that the amine−epoxy reaction is a suitable path to create bonds in these, and future, nonlinear radical macromolecules. In turn, this reaction system presents itself as a clear means by which to synthesize future dendrimers with higher generation levels and, thus, elevated radical content.

To better elucidate the nanoscale structure−property relationships of these three-armed radical macromolecules in terms of their spin and charge transport potential, simulations focusing on the radical distribution of E1-TEMPO were completed. These simulations included comparisons of the radical dendrimer at temperatures below and above the glass transition temperature to investigate whether a significant configurational change accompanies heating above T_g, as has been hypothesized to occur within PTEO. The conformations and packing of radical dendrimers were evaluated by a combination of the conformer ensemble search tool (CREST)[66,67] and GFN-FF based molecular dynamics simulations.[74] The spin-density isosurface (Figure 3b) of the lowest energy conformer discovered by CREST points toward the idea that the nitroxide groups are distributed around the outer surface of E1-TEMPO without sufficient conformational freedom with which to closely associate. This suggests that spin transport and charge transport would be dominated by peripheral transfer paths around the macromolecule core (at least at 0 K in this minimum energy structure). The radical configurations at finite temperatures were subsequently evaluated by performing MD simulations at temperatures 20 K greater than and less than the experimentally established glass transition temperature (i.e., the simulations were performed at temperatures of 233 and 273 K). The nitrogen−oxygen radial distribution function (RDF) maxima of the radical-containing macromolecules occurs at approximately 5 and 7.5 Å (Figure 3c), which is similar to the case of an earlier MD study of the linear radical polymer poly(2,2,6,6-tetramethylpiperidinyloxy methacrylate) (PTMA).[75] A subtle

https://doi.org/10.1021/acspolymersau.1c00026
ACS Polym. Au 2022, 2, 59−68

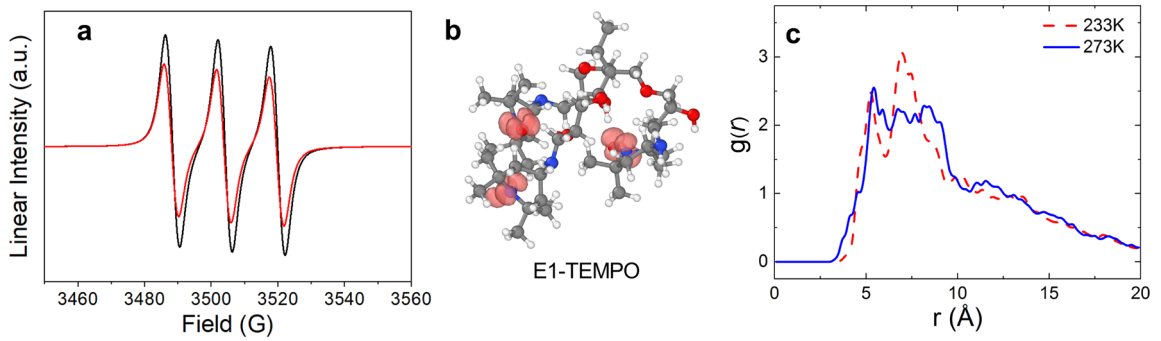

Figure 3. (a) Linear EPR spectrum of E1-TEMPO (red) showing the typical triplet signals in same shape as those seen in the EPR spectrum of 4-amino-TEMPO (black). These data highlight that the intramolecular spin interactions do not occur in the nonlinear radical macromolecule. (b) Spin density visualization of E1-TEMPO at the lowest energy state as observed by CREST where the atoms are represented by the following colors: C, gray; O, red; N, blue; H, white. (c) RDF plot of the nitrogen−oxygen atom within E1-TEMPO were based on GFN-FF molecular dynamics simulations calculated at temperatures of 273 and 233 K.

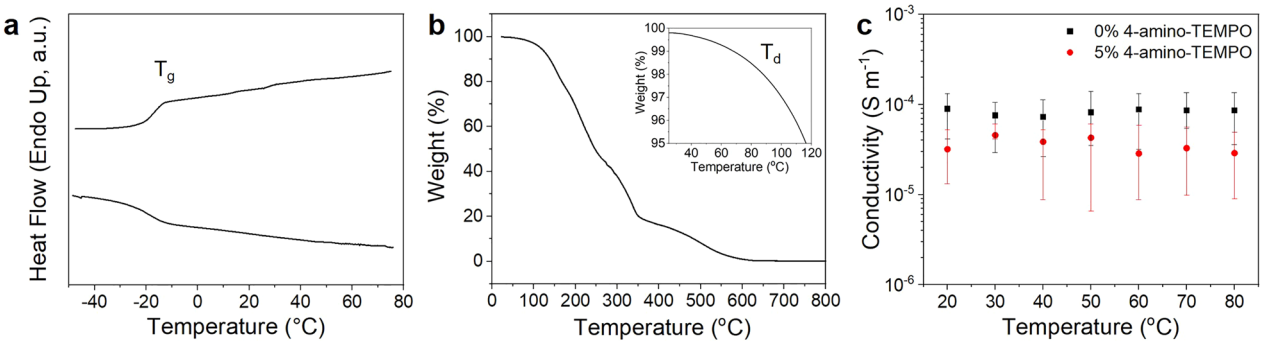

Figure 4. (a) The glass transition temperature of E1-TEMPO is about −20 °C, as determined by DSC. (b) The onset degradation temperature of E1-TEMPO is ∼96 °C. (c) Electrical conductivity tests were performed in the temperature range of 20−80 °C in intervals of 10 °C for the pristine (i.e., not doped) E1-TEMPO thin films (black squares) and E1-TEMPO thin films that included small molecule additives at 5% (by weight) as well (red circles).

change of configurational energy and a shorter RDF at the temperature below T_g were observed, which indicates that the nonlinear radical macromolecule is packed in a slightly denser configuration as it enters the glassy state. There is a double peak signature (6 and 8 Å) at both temperatures, which corresponds to nitroxide groups in head-to-head vs methyl-spacing slipped configurations, respectively. Interestingly, this distribution shifts with respect to temperature, although we cannot comment at this stage on its potential impact on the macroscopic conductivity.

After confirming that E1-TEMPO was successfully synthesized as a well-defined molecule with high radical content, and with the support of computational results showing radicals facing the outside of the surface of the macromolecule, we anticipated that the material would have unique electronic and magnetic properties. Consistent with our previous observation regarding high-conductivity linear radical polymers, we aimed for this nonlinear radical macromolecule to have a relatively low (i.e., below room temperature) glass transition temperature. This was achieved as the T_g of E1-TEMPO is −20 °C (Figure 4a), which is >100 °C removed from its onset degradation temperature of ∼96 °C (Figure 4b). This large window offers a clear path to optimize the processing of the material, and it affords a means by which to evaluate any thermally activated transport properties of the macromolecule. In fact, the conductivity value of pristine E1-TEMPO was $\sim 10^{-4}$ S m^{-1}, temperature independent across the temperatures evaluated here, and approximately the same as that of many linear nonconjugated radical polymers (Figure 4c). This corresponds to the similar peak positions of the simulated nitrogen−oxygen RDF near the experimentally measured glass transition temperature. Additionally, to observe the difference when dopants were added, we also measured the conductivity of E1-TEMPO thin films containing 5% 4-amino-TEMPO, which was added to decrease the average radical−radical spacing within the thin film. Counterintuitively, the conductivity values did not change (or slightly decreased) when 4-amino-TEMPO was added, suggesting that the addition of the small molecule radical species did not increase radical−radical interactions. Unfortunately, we were unable to add larger loadings of the small molecule to the radical dendrimer thin film as larger loadings significantly decreased the quality of the thin film. Moreover, in a manner that is distinct from its low-T_g linear polymer analogue (PTEO), the radical−radical coupling in the solid state is not as large as that of the corresponding linear radical polymer. This highlights the need to have significant nitroxide−nitroxide interactions when thin films are cast if high electrical conductivity values are to be had in radical macromolecule systems, and it suggests that increasing the number of generations in nonlinear radical macromolecules could play a key role in increasing radical−radical interactions.

In terms of the magnetic properties of the radical dendrimer, the high-temperature interactions between the unpaired electrons of E1-TEMPO demonstrated typical paramagnetic behavior. For paramagnetic materials, the thermal energy of the system prevents the spins from ordering with the applied

https://doi.org/10.1021/acspolymersau.1c00026
ACS Polym. Au 2022, 2, 59−68

magnetic field. Therefore, decreasing the temperature allows for the spins to align to the applied magnetic field and the magnetic susceptibility of the system increases (Figure 5a).

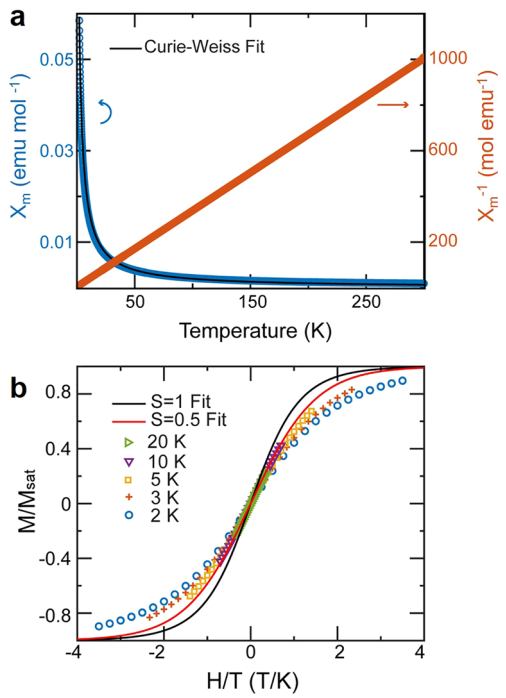

Figure 5. (a) Magnetic susceptibility tests were performed using an applied field of 0.5 T with a temperature ranging from 2 to 300 K on E1-TEMPO. E1-TEMPO displayed typical paramagnetic behavior which was fit to a Curie−Weiss model. (b) Magnetization curves were fit to a Brillouin curve for $S = 0.5$. As the temperature decreased, the magnetization curves for E1-TEMPO diverged from the curve, indicating weak antiferromagnetic interactions between the unpaired electrons.

The magnetic susceptibility of E1-TEMPO was corrected for the contribution of the diamagnetic susceptibility. Using Pascal's constants,[76] the diamagnetic susceptibility of E1-TEMPO was -5.7×10^{-4} emu mol^{-1}. The molar magnetic susceptibility was then fit to the Curie−Weiss law, as described by eq 1.

$$\chi_m = \frac{C}{T - \theta} \tag{1}$$

Here, C is the Curie constant and θ is the Curie temperature. The Curie constant was about 0.19, θ was −1.38 K, and the molar magnetic susceptibility, χ_m, was 5.85×10^{-2} emu mol^{-1} at 2 K and 9.35×10^{-4} emu mol^{-1} at 300 K. This value is less than expected, as theoretically, χ_m at 300 K for an unpaired electron is 1.25×10^{-3} emu mol^{-1}.[8] This disparity between the measured and theoretical magnetic susceptibility is due to the 85% radical content of E1-TEMPO, consistent with the EPR data shown above.

This behavior can be furthered explained by measuring the effective magnetic moment, μ_{eff}, according to eq 2.

$$\mu_{eff} = 2.828(\chi_m T)^{1/2} \tag{2}$$

For a paramagnetic material with a single unpaired electron (e.g., the nitroxide radical), μ_{eff} is expected to be 1.73 μ_b, where μ_b is the Bohr magneton (5.8×10^{-4} eV T^{-1}), and independent of temperature. However, at 300 K, the μ_{eff} of E1-TEMPO is 1.49 μ_b, and at 2 K it decreases to 0.97μ_b (Figure S4). Comparing the room temperature μ_{eff} of E1-TEMPO to the theoretical value of 1.73μ_b yields a radical content of 85%, again consistent with the EPR measurements. Furthermore, this sharp decrease in the magnitude of μ_{eff} indicated antiferromagnetic interactions between the unpaired electrons. The idea that these were antiferromagnetic interactions was further supported based on the results of magnetization measurements. When a high field is applied to a paramagnet, all the spins of the system align to the field and the measured magnetization asymptotes to a value of M_{sat}. For E1-TEMPO, M_{sat} was 2172 emu mol^{-1}. The magnetization behavior of the paramagnetic system can then be modeled using a Brillouin function, $B_s(x)$, where the following equations hold.

$$M = M_{sat} B_s(x) \tag{3}$$

Here,

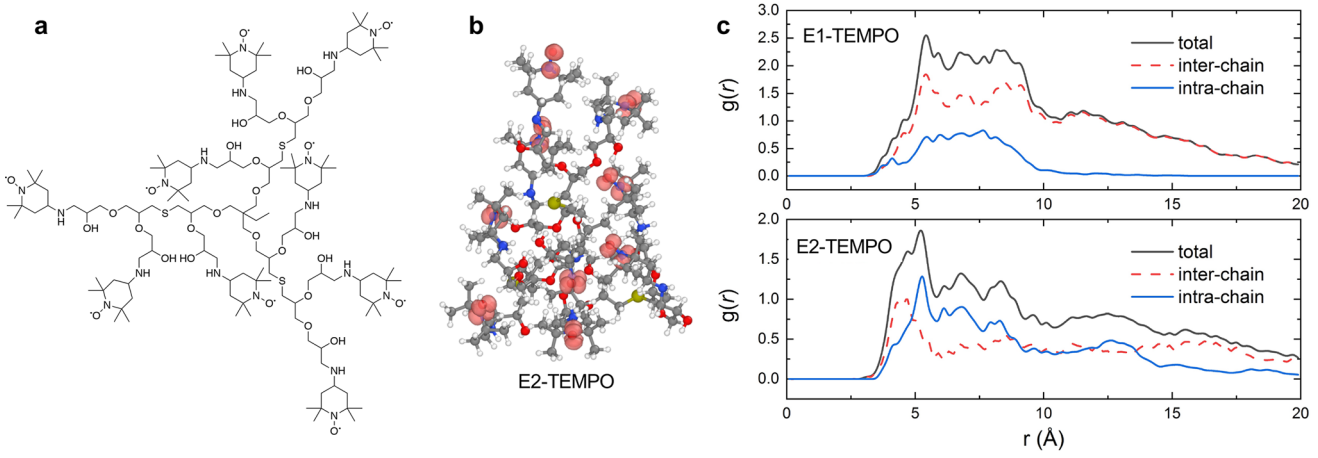

Figure 6. (a) Chemical structure of a second-generation dendrimer, E2-TEMPO. (b) Spin density visualization of the lowest energy CREST conformer where the atoms are represented by the following colors: C, gray; O, red; N, blue; H, white. (c) Interchain and intrachain RDFs of E1-TEMPO (upper) and E2-TEMPO (lower). Nitrogen−oxygen atoms were computed in GFN-FF based molecular dynamics simulations at 273 K.

https://doi.org/10.1021/acspolymersau.1c00026
ACS Polym. Au 2022, 2, 59−68

$$B_s(x) = \frac{2S+1}{2S}\coth\left(\frac{2S+1}{2S}x\right) - \frac{1}{2S}\coth\left(\frac{1}{2S}x\right) \quad (4)$$

and

$$x = \frac{gS\mu_B H}{k_B T} \quad (5)$$

where g is the g-factor and S is the electron spin quantum number. The magnetization behavior of E1-TEMPO was then fit to eq 3 using M_{sat} as the fitting parameter while keeping the value of S fixed for all of the temperatures evaluated.

The Brillouin function models the behavior of a paramagnet without any interactions between the spins.[77] Because the nitroxide radical has a single unpaired electron, the measured magnetization curves should fit the Brillouin curve for an S value of 0.5 (Figure 5b). However, as the temperature decreased to less than 10 K, the curves diverged downward from the expected values. This deviation from the predicted behavior is consistent with the presence of antiferromagnetic interactions.[78−80] This antiferromagnetic behavior has previously been seen in similar amorphous materials containing nitroxide radicals.[42,44,81] In this way, E1-TEMPO shows great promise as a magnetically active radical dendrimer, and further work on its structure−property relationships will further strengthen these spin interactions.

Although the focus to this point has been on the first generation radical dendrimer, E1-TEMPO, the natural next step is to investigate the impact of pursuing higher-generation synthetic targets. Even though steric hindrance of the functional groups will increase with increasing dendrimer generations, prior efforts that have focused on dendrimer syntheses using this particular series of reactions demonstrated that the creation of third- or fourth-generation dendrimers is possible.[82,83] To establish the potential utility of synthesizing higher generation dendrimers in the future, we performed conformational sampling and MD simulations of the second-generation dendrimer species E2-TEMPO (Figure 6a) that were analogous to those reported for E1-TEMPO. Based on the lowest energy conformer discovered by CREST (Figure 6b), the nitroxide groups are distributed at the outside surface of the second-generation dendrimer similar to what was observed in the case of E1-TEMPO. In comparing the RDF between two generations of dendrimers, a slight shift to lower distances with respect to the total nitrogen−nitrogen, nitrogen−oxygen, and oxygen−oxygen RDF was observed for the higher generation dendrimer (Figure S5). These lower distance values would directly imply a higher density of open-shell units, leading to more spin−spin interaction pathways. To distinguish between radical−radical interactions between dendrimers (inter) and within the same dendrimer (intra), the corresponding radical RDFs were analyzed separately (Figure 6c). The reduction of the peak intrachain separation within the higher generation dendrimer indicates an increased surface density of nitroxides when the dendritic structure grows higher and suggests that charge transport shifts from interchain to intrachain. Due to the shorter distance of intramolecular interactions compared to intermolecular interaction, denser packing and stronger spin−spin coupling characteristics are also expected for multiple-generation radical dendrimers. Although the current conductivity values of E1-TEMPO are not significantly enhanced compared to earlier reported open-shell linear polymers, computational results point toward the idea that higher generation open-shell dendrimers could be advantageous in terms of combining linear radical polymer and dendritic closed-shell macromolecule designs.

CONCLUSIONS

A three-arm nonconjugated radical macromolecule, E1-TEMPO, was synthesized through a one-step amine−epoxy ring-opening reaction to yield a macromolecule with a well-defined molecular weight and arrow molecular weight distribution. Importantly, the metal-free reaction scheme utilized had no noticeable side reactions such that a well-defined macromolecule with a relatively high radical content was generated. Moreover, the design of the backbone arms of the macromolecule resulted in a material with a low glass transition temperature that was amorphous in the solid state. In turn, this afforded a material with a reasonable electronic conductivity and magnetic properties that displayed a paramagnetic-to-antiferromagnetic transition at <10 K. This antiferromagnetic behavior arose because of spin−spin interactions in the locally ordered neighbor radicals within the nonlinear radical macromolecule sample, which computational simulations suggest could be increased by increasing the number of generations associated with the dendritic open-shell structure. Through this polymeric design and demonstration of its magnetoelectronic properties, this effort provides a clear first step toward future designs of advanced nonlinear nonconjugated radical macromolecules.

ASSOCIATED CONTENT

Supporting Information

The Supporting Information is available free of charge at https://pubs.acs.org/doi/10.1021/acspolymersau.1c00026.

Reaction scheme for the synthesis of the nonlinear radical macromolecule; ^{13}C NMR spectrum and EPR spectroscopy data of the nonlinear radical macromolecule; temperature-dependent μ_{eff} data; simulation results of the E2-TEMPO macromolecule (PDF)

AUTHOR INFORMATION

Corresponding Author

Bryan W. Boudouris − *Charles D. Davidson School of Chemical Engineering and Department of Chemistry, Purdue University, West Lafayette, Indiana 47907, United States;* orcid.org/0000-0003-0428-631X; Email: boudouris@purdue.edu

Authors

Hyunki Yeo − *Charles D. Davidson School of Chemical Engineering, Purdue University, West Lafayette, Indiana 47907, United States*

Siddhartha Akkiraju − *Charles D. Davidson School of Chemical Engineering, Purdue University, West Lafayette, Indiana 47907, United States*

Ying Tan − *Charles D. Davidson School of Chemical Engineering, Purdue University, West Lafayette, Indiana 47907, United States;* orcid.org/0000-0002-7762-0836

Hamas Tahir − *Charles D. Davidson School of Chemical Engineering, Purdue University, West Lafayette, Indiana 47907, United States*

Neil R. Dilley − *Birck Nanotechnology Center, Purdue University, West Lafayette, Indiana 47907, United States*

https://doi.org/10.1021/acspolymersau.1c00026
ACS Polym. Au 2022, 2, 59−68

Brett M. Savoie − *Charles D. Davidson School of Chemical Engineering, Purdue University, West Lafayette, Indiana 47907, United States;* orcid.org/0000-0002-7039-4039

Complete contact information is available at: https://pubs.acs.org/10.1021/acspolymersau.1c00026

Notes

The authors declare no competing financial interest.

■ ACKNOWLEDGMENTS

This work was supported by the U.S. Department of Energy, Office of Science, Basic Energy Sciences, under Award DE-SC0021967 (Program Manager: Dr. Michael Sennett). We thank the Department of Energy for this generous support.

■ REFERENCES

(1) Kelley, T. W.; Baude, P. F.; Gerlach, C.; Ender, D. E.; Muyres, D.; Haase, M. A.; Vogel, D. E.; Theiss, S. D. Recent Progress in Organic Electronics: Materials, Devices, and Processes. *Chem. Mater.* **2004**, *16* (23), 4413−4422.

(2) Xie, J.; Gu, P.; Zhang, Q. Nanostructured Conjugated Polymers: Toward High-Performance Organic Electrodes for Rechargeable Batteries. *ACS Energy Lett.* **2017**, *2* (9), 1985−1996.

(3) Ma, H.; Yip, H. L.; Huang, F.; Jen, A. K. Y. Interface Engineering for Organic Electronics. *Adv. Funct. Mater.* **2010**, *20* (9), 1371−1388.

(4) Nezakati, T.; Seifalian, A.; Tan, A.; Seifalian, A. M. Conductive Polymers: Opportunities and Challenges in Biomedical Applications. *Chem. Rev.* **2018**, *118* (14), 6766−6843.

(5) Moliton, A.; Hiorns, R. C. Review of Electronic and Optical Properties of Semiconducting π-Conjugated Polymers: Applications in Optoelectronics. *Polym. Int.* **2004**, *53* (10), 1397−1412.

(6) Akkiraju, S.; Vergados, J.; Hoagland, L.; Lu, Z.; Anandan, V.; Boudouris, B. W. Design of Mixed Electron- And Ion-Conducting Radical Polymer-Based Blends. *Macromolecules* **2021**, *54* (11), 5178−5186.

(7) McQuade, D. T.; Pullen, A. E.; Swager, T. M. Conjugated Polymer-Based Chemical Sensors. *Chem. Rev.* **2000**, *100* (7), 2537−2574.

(8) Günes, S.; Neugebauer, H.; Sariciftci, N. S. Conjugated Polymer-Based Organic Solar Cells. *Chem. Rev.* **2007**, *107* (4), 1324−1338.

(9) Coakley, K. M.; McGehee, M. D. Conjugated Polymer Photovoltaic Cells. *Chem. Mater.* **2004**, *16* (23), 4533−4542.

(10) Tuncel, D.; Demir, H. V. Conjugated Polymer Nanoparticles. *Nanoscale* **2010**, *2* (4), 484−494.

(11) Lee, S.; Kwon, G.; Ku, K.; Yoon, K.; Jung, S. K.; Lim, H. D.; Kang, K. Recent Progress in Organic Electrodes for Li and Na Rechargeable Batteries. *Adv. Mater.* **2018**, *30* (42), 1704682.

(12) Solak, A. O.; Eichorst, L. R.; Clark, W. J.; McCreery, R. L. Modified Carbon Surfaces as "Organic Electrodes" That Exhibit Conductance Switching. *Anal. Chem.* **2003**, *75* (2), 296−305.

(13) Inal, S.; Rivnay, J.; Suiu, A.-O.; Malliaras, G. G.; McCulloch, I. Conjugated Polymers in Bioelectronics. *Acc. Chem. Res.* **2018**, *51* (6), 1368−1376.

(14) Schwartz, G.; Tee, B. C.-K.; Mei, J.; Appleton, A. L.; Kim, D. H.; Wang, H.; Bao, Z. Flexible Polymer Transistors with High Pressure Sensitivity for Application in Electronic Skin and Health Monitoring. *Nat. Commun.* **2013**, *4* (1), 1859.

(15) Guo, X.; Baumgarten, M.; Müllen, K. Designing π-Conjugated Polymers for Organic Electronics. *Prog. Polym. Sci.* **2013**, *38* (12), 1832−1908.

(16) Feng, L.; Zhu, C.; Yuan, H.; Liu, L.; Lv, F.; Wang, S. Conjugated Polymer Nanoparticles: Preparation, Properties, Functionalization and Biological Applications. *Chem. Soc. Rev.* **2013**, *42* (16), 6620−6633.

(17) L. Villaraza, A. J.; Bumb, A.; Brechbiel, M. W. Macromolecules, Dendrimers, and Nanomaterials in Magnetic Resonance Imaging: The Interplay between Size, Function, and Pharmacokinetics. *Chem. Rev.* **2010**, *110* (5), 2921−2959.

(18) Kumar, S.; Kumar, Y.; Keshri, S.; Mukhopadhyay, P. Recent Advances in Organic Radicals and Their Magnetism. *Magnetochemistry* **2016**, *2* (4), 42.

(19) Iwamura, H. What Role Has Organic Chemistry Played in the Development of Molecule-Based Magnets? *Polyhedron* **2013**, *66*, 3−14.

(20) Lutkenhaus, J. A Radical Advance for Conducting Polymers. *Science (Washington, DC, U. S.)* **2018**, *359* (6382), 1334−1335.

(21) Wang, S.; Li, F.; Easley, A. D.; Lutkenhaus, J. L. Real-Time Insight into the Doping Mechanism of Redox-Active Organic Radical Polymers. *Nat. Mater.* **2019**, *18* (1), 69−75.

(22) Rajca, A. Organic Diradicals and Polyradicals: From Spin Coupling to Magnetism? *Chem. Rev.* **1994**, *94* (4), 871−893.

(23) Rajca, A.; Utamapanya, S. Poly(Arylmethyl) Quartet Triradicals and Quintet Tetraradicals. *J. Am. Chem. Soc.* **1993**, *115* (6), 2396−2401.

(24) Rajca, A. Toward Organic Synthesis of a Nanometer-size Magnetic Particle. *Adv. Mater.* **1994**, *6* (7−8), 605−607.

(25) Rajca, A.; Wongsriratanakul, J.; Rajca, S.; Cerny, R. A Dendritic Macrocyclic Organic Polyradical with a Very High Spin of S = 10. *Angew. Chem., Int. Ed.* **1998**, *37* (9), 1229−1232.

(26) Rajca, A.; Utamapanya, S.; Smithhisler, D. J. Near-Degeneracy between the Low- and High-Spin States in an Alternant Hydrocarbon Diradical: Topology and Geometry. *J. Org. Chem.* **1993**, *58* (21), 5650−5652.

(27) Rajca, A. The Physical Organic Chemistry of Very High-Spin Polyradicals. *Adv. Phys. Org. Chem.* **2005**, *40* (05), 153−199.

(28) Zhang, K.; Monteiro, M. J.; Jia, Z. Stable Organic Radical Polymers: Synthesis and Applications. *Polym. Chem.* **2016**, *7* (36), 5589−5614.

(29) Oyaizu, K.; Nishide, H. Radical Polymers for Organic Electronic Devices: A Radical Departure from Conjugated Polymers? *Adv. Mater.* **2009**, *21* (22), 2339−2344.

(30) Chung, J.; Khot, A.; Savoie, B. M.; Boudouris, B. W. 100th Anniversary of Macromolecular Science Viewpoint: Recent Advances and Opportunities for Mixed Ion and Charge Conducting Polymers. *ACS Macro Lett.* **2020**, *9* (5), 646−655.

(31) Wingate, A. J.; Boudouris, B. W. Recent Advances in the Syntheses of Radical-Containing Macromolecules. *J. Polym. Sci., Part A: Polym. Chem.* **2016**, *54* (13), 1875−1894.

(32) Wilcox, D. A.; Agarkar, V.; Mukherjee, S.; Boudouris, B. W. Stable Radical Materials for Energy Applications. *Annu. Rev. Chem. Biomol. Eng.* **2018**, *9* (1), 83−103.

(33) Mukherjee, S.; Boudouris, B. W. *Applications of Radical Polymers in Solid-State Devices*; Springer, 2017.

(34) Abe, M. Diradicals. *Chem. Rev.* **2013**, *113*, 7011−7088.

(35) Badetti, E.; Lloveras, V.; Amadio, E.; Di Lorenzo, R.; Olivares-Marín, M.; Tesio, A. Y.; Zhang, S.; Pan, F.; Rissanen, K.; Veciana, J.; Tonti, D.; Vidal-Gancedo, J.; Zonta, C.; Licini, G. Organic Polyradicals as Redox Mediators: Effect of Intramolecular Radical Interactions on Their Efficiency. *ACS Appl. Mater. Interfaces* **2020**, *12* (41), 45968.

(36) Li, F.; Zhang, Y.; Kwon, S. R.; Lutkenhaus, J. L. Electropolymerized Polythiophenes Bearing Pendant Nitroxide Radicals. *ACS Macro Lett.* **2016**, *5* (3), 337−341.

(37) Endo, T.; Takuma, K.; Takata, T.; Hirose, C. Synthesis and Polymerization of 4-(Glycidyloxy)-2,2,6,6-Tetramethylpiperidine-1-Oxyl. *Macromolecules* **1993**, *26* (12), 3227−3229.

(38) Li, F.; Zhang, Y.; Kwon, S. R.; Lutkenhaus, J. L. Electropolymerized Polythiophenes Bearing Pendant Nitroxide Radicals. *ACS Macro Lett.* **2016**, *5* (3), 337−341.

(39) Nguyen, T. P.; Easley, A. D.; Kang, N.; Khan, S.; Lim, S.-M.; Rezenom, Y. H.; Wang, S.; Tran, D. K.; Fan, J.; Letteri, R. A.; He, X.; Su, L.; Yu, C.-H.; Lutkenhaus, J. L.; Wooley, K. L. Polypeptide Organic Radical Batteries. *Nature* **2021**, *593* (7857), 61−66.

(40) Mike, J. F.; Lutkenhaus, J. L. Electrochemically Active Polymers for Electrochemical Energy Storage: Opportunities and Challenges. *ACS Macro Lett.* **2013**, *2* (9), 839−844.
(41) Nakahara, K.; Iwasa, S.; Satoh, M.; Morioka, Y.; Iriyama, J.; Suguro, M.; Hasegawa, E. Rechargeable Batteries with Organic Radical Cathodes. *Chem. Phys. Lett.* **2002**, *359* (5), 351−354.
(42) Kamachi, M.; Tamaki, M.; Morishima, Y.; Nozakura, S.; Mori, W.; Kishita, M. Electron Exchange Phenomena of Polymers Containing Nitroxyl Radicals. *Polym. J.* **1982**, *14* (5), 363−369.
(43) Nozakura, S.; Kamachi, M. Magnetic Properties of Polymers Containing Paramagnetic Species. *Makromol. Chem.* **1985**, *12* (S19851), 255−263.
(44) Kamachi, M.; Enomoto, H.; Shibasaka, M.; Mori, W.; Kishita, M. Magnetic Properties of Polymer Containing Verdazyl in the Side Chain. *Polym. J.* **1986**, *18* (5), 439−441.
(45) Zhang, Y.; Park, A. M.; McMillan, S. R.; Harmon, N. J.; Flatté, M. E.; Fuchs, G. D.; Ober, C. K. Charge Transport in Conjugated Polymers with Pendent Stable Radical Groups. *Chem. Mater.* **2018**, *30* (14), 4799−4807.
(46) Zhang, Y.; Park, A.; Cintora, A.; McMillan, S. R.; Harmon, N. J.; Moehle, A.; Flatté, M. E.; Fuchs, G. D.; Ober, C. K. Impact of the Synthesis Method on the Solid-State Charge Transport of Radical Polymers. *J. Mater. Chem. C* **2018**, *6* (1), 111−118.
(47) Bugnon, L.; Morton, C. J. H.; Novak, P.; Vetter, J.; Nesvadba, P. Synthesis of Poly(4-Methacryloyloxy-TEMPO) via Group-Transfer Polymerization and Its Evaluation in Organic Radical Battery. *Chem. Mater.* **2007**, *19* (11), 2910−2914.
(48) Tan, Y.; Casetti, N. C.; Boudouris, B. W.; Savoie, B. M. Molecular Design Features for Charge Transport in Nonconjugated Radical Polymers. *J. Am. Chem. Soc.* **2021**, *143* (31), 11994−12002.
(49) Hay, M. E.; Hui Wong, S.; Mukherjee, S.; Boudouris, B. W. Controlling Open-Shell Loading in Norbornene-Based Radical Polymers Modulates the Solid-State Charge Transport Exponentially. *J. Polym. Sci., Part B: Polym. Phys.* **2017**, *55* (20), 1516−1525.
(50) Joo, Y.; Agarkar, V.; Sung, S. H.; Savoie, B. M.; Boudouris, B. W. A Nonconjugated Radical Polymer Glass with High Electrical Conductivity. *Science (Washington, DC, U. S.)* **2018**, *359* (6382), 1391−1395.
(51) Gadwal, I.; Khan, A. Multiply Functionalized Dendrimers: Protective-Group-Free Synthesis through Sequential Thiol-Epoxy "click" Chemistry and Esterification Reaction. *RSC Adv.* **2015**, *5* (55), 43961−43964.
(52) Sato, K.; Sukegawa, T.; Oyaizu, K.; Nishide, H. Synthesis of Poly(TEMPO-Substituted Glycidyl Ether) by Utilizing t-BuOK/18-Crown-6 for an Organic Cathode-Active Material. *Macromol. Symp.* **2015**, *351* (1), 90−96.
(53) Badetti, E.; Lloveras, V.; Muñoz-Gómez, J. L.; Sebastián, R. M.; Caminade, A. M.; Majoral, J. P.; Veciana, J.; Vidal-Gancedo, J. Radical Dendrimers: A Family of Five Generations of Phosphorus Dendrimers Functionalized with TEMPO Radicals. *Macromolecules* **2014**, *47* (22), 7717−7724.
(54) Mohamad Ali, B.; Velavan, B.; Sudhandiran, G.; Sridevi, J.; Sultan Nasar, A. Radical Dendrimers: Synthesis, Anti-Tumor Activity and Enhanced Cytoprotective Performance of TEMPO Free Radical Functionalized Polyurethane Dendrimers. *Eur. Polym. J.* **2020**, *122* (November 2019), 109354.
(55) Duncan, R.; Izzo, L. Dendrimer Biocompatibility and Toxicity. *Adv. Drug Delivery Rev.* **2005**, *57* (15), 2215−2237.
(56) Pan, B. F.; Gao, F.; Ao, L. M. Investigation of Interactions between Dendrimer-Coated Magnetite Nanoparticles and Bovine Serum Albumin. *J. Magn. Magn. Mater.* **2005**, *293* (1), 252−258.
(57) Chandra, S.; Patel, M. D.; Lang, H.; Bahadur, D. Dendrimer-Functionalized Magnetic Nanoparticles: A New Electrode Material for Electrochemical Energy Storage Devices. *J. Power Sources* **2015**, *280*, 217−226.
(58) Smalberg, F.; Moulijn, J.; van Bekkum, H. Feature Article. *Green Chem.* **2000**, *2* (6), G97−G100.
(59) Hong, J.; Khan, A. Thermoresponsive poly(β-hydroxyl amine)s: Synthesis of a new stimuli responsive amphiphilic homopolymer family through amine-epoxy 'click' polymerization. *Polymers* **2019**, *11* (12), 1941.
(60) Oh, J.; Jung, K. I.; Jung, H. W.; Khan, A. A Modular and Practical Synthesis of Zwitterionic Hydrogels through Sequential Amine-Epoxy "Click" Chemistry and N-Alkylation Reaction. *Polymers (Basel, Switz.)* **2019**, *11* (9), 1491.
(61) Yeo, H.; Khan, A. Photoinduced Proton-Transfer Polymerization: A Practical Synthetic Tool for Soft Lithography Applications. *J. Am. Chem. Soc.* **2020**, *142* (7), 3479−3488.
(62) Doszlop, S.; Vargha, V.; Horkay, F. Reactions of Epoxy With Other Functional Groups and the Arising Sec-Hydroxyl Groups. *Period. Polytech., Chem. Eng.* **1978**, *22* (3), 253−275.
(63) Baradwaj, A. G.; Wong, S. H.; Laster, J. S.; Wingate, A. J.; Hay, M. E.; Boudouris, B. W. Impact of the Addition of Redox-Active Salts on the Charge Transport Ability of Radical Polymer Thin Films. *Macromolecules* **2016**, *49* (13), 4784−4791.
(64) He, J.; Mukherjee, S.; Zhu, X.; You, L.; Boudouris, B. W.; Mei, J. Highly Transparent Crosslinkable Radical Copolymer Thin Film as the Ion Storage Layer in Organic Electrochromic Devices. *ACS Appl. Mater. Interfaces* **2018**, *10* (22), 18956−18963.
(65) Rostro, L.; Baradwaj, A. G.; Boudouris, B. W. Controlled Radical Polymerization and Quantification of Solid State Electrical Conductivities of Macromolecules Bearing Pendant Stable Radical Groups. *ACS Appl. Mater. Interfaces* **2013**, *5* (20), 9896−9901.
(66) Grimme, S. Exploration of Chemical Compound, Conformer, and Reaction Space with Meta-Dynamics Simulations Based on Tight-Binding Quantum Chemical Calculations. *J. Chem. Theory Comput.* **2019**, *15* (5), 2847−2862.
(67) Pracht, P.; Bohle, F.; Grimme, S. Automated Exploration of the Low-Energy Chemical Space with Fast Quantum Chemical Methods. *Phys. Chem. Chem. Phys.* **2020**, *22* (14), 7169−7192.
(68) Spicher, S.; Grimme, S. Robust Atomistic Modeling of Materials, Organometallic, and Biochemical Systems. *Angew. Chem.* **2020**, *132* (36), 15795−15803.
(69) Rappé, A. K.; Casewit, C. J.; Colwell, K. S.; Goddard, W. A.; Skiff, W. M. UFF, a Full Periodic Table Force Field for Molecular Mechanics and Molecular Dynamics Simulations. *J. Am. Chem. Soc.* **1992**, *114* (25), 10024−10035.
(70) Hanwell, M. D.; Curtis, D. E.; Lonie, D. C.; Vandermeersch, T.; Zurek, E.; Hutchison, G. R. Avogadro: An Advanced Semantic Chemical Editor, Visualization, and Analysis Platform. *J. Cheminf.* **2012**, *4*, 17.
(71) Bannwarth, C.; Ehlert, S.; Grimme, S. GFN2-XTB - An Accurate and Broadly Parametrized Self-Consistent Tight-Binding Quantum Chemical Method with Multipole Electrostatics and Density-Dependent Dispersion Contributions. *J. Chem. Theory Comput.* **2019**, *15* (3), 1652−1671.
(72) Tomlinson, E. P.; Hay, M. E.; Boudouris, B. W. Radical Polymers and Their Application to Organic Electronic Devices. *Macromolecules* **2014**, *47* (18), 6145−6158.
(73) Huang, G.; Daiguebonne, C.; Calvez, G.; Suffren, Y.; Guillou, O.; Guizouarn, T.; Le Guennic, B.; Cador, O.; Bernot, K. Strong Magnetic Coupling and Single-Molecule-Magnet Behavior in Lanthanide-TEMPO Radical Chains. *Inorg. Chem.* **2018**, *57* (17), 11044−11057.
(74) Spicher, S.; Grimme, S. Robust Atomistic Modeling of Materials,Organometallic, and Biochemical Systems. *Angew. Chem., Int. Ed.* **2020**, *59*, 15665−15673.
(75) Kemper, T. W.; Larsen, R. E.; Gennett, T. Relationship between Molecular Structure and Electron Transfer in a Polymeric Nitroxyl-Radical Energy Storage Material. *J. Phys. Chem. C* **2014**, *118*, 17213−17220.
(76) Bain, G. A.; Berry, J. F. Diamagnetic Corrections and Pascal's Constants. *J. Chem. Educ.* **2008**, *85* (4), 532−536.
(77) Kittel, C. *Introduction to Solid State Physics*, 5th ed.; Wiley, 1976.
(78) Tomioka, K.; Mitsubori, S.; Ishida, T.; Nogami, T.; Iwamura, H. Intermolecular Ferromagnetic Interaction of 4-Benzylideneamino-

https://doi.org/10.1021/acspolymersau.1c00026
ACS Polym. Au 2022, 2, 59−68

2, 2, 6, 6-Tetramethylpiperidin-1-Oxyl. *Chem. Lett.* **1993**, *22* (7), 1239−1242.
(79) Nogami, T.; Tomioka, K.; Ishida, T.; Yoshikawa, H.; Yasui, M.; Iwasaki, F.; Iwamura, H.; Takeda, N.; Ishikawa, M. A New Organic Ferromagnet: 4-Benzylideneamino-2, 2, 6, 6-Tetramethylpiperidin-1-Oxyl. *Chem. Lett.* **1994**, *23* (1), 29−32.
(80) Zając, M.; Gosk, J.; Kamińska, M.; Twardowski, A.; Szyszko, T.; Podsiadło, S. Paramagnetism and Antiferromagnetic d−d Coupling in GaMnN Magnetic Semiconductor. *Appl. Phys. Lett.* **2001**, *79* (15), 2432−2434.
(81) Allgaier, J.; Finkelmann, H. Anionic Polymerization of 4-Methacryloyloxy-2,2,6,6-Tetramethylpiperidin-1-Oxyl and the Magnetic Properties of the Polymer. *Makromol. Chem., Rapid Commun.* **1993**, *14* (5), 267−271.
(82) Killops, K. L.; Campos, L. M.; Hawker, C. J. Robust, Efficient, and Orthogonal Synthesis of Dendrimers via Thiol-Ene "Click" Chemistry. *J. Am. Chem. Soc.* **2008**, *130* (15), 5062−5064.
(83) Hawker, C. J.; Frechet, J. M. J. Preparation of Polymers with Controlled Molecular Architecture. A New Convergent Approach to Dendritic Macromolecules. *J. Am. Chem. Soc.* **1990**, *112* (21), 7638−7647.

https://doi.org/10.1021/acspolymersau.1c00026
ACS Polym. Au 2022, 2, 59−68